1968

# Effect of single peak overloading on fatigue crack propagation

Eric F. J. von Euw
*Lehigh University*

# EFFECT OF SINGLE PEAK OVERLOADING ON FATIGUE CRACK PROPAGATION

by

Eric F.J. von Euw

A Thesis

Presented to the Graduate Committee

of Lehigh University

in Candidacy for the Degree of

Master of Science

in

Mechanical Engineering

Lehigh University

1968

## Certificate of Approval

This thesis is accepted and approved in partial fulfillment of the requirements for the degree of Master of Science.

September 13, 1968
(Date)

Richard W Hertzberg
Thesis Advisor
Professor Richard W. Hertzberg

Richard Roberts
Department Advisor
Professor Richard Roberts

Ferdinand P. Beer
Head of the Department
Professor Ferdinand Beer

## ACKNOWLEDGMENTS

The patience, guidance and instruction of Professor Richard W. Hertzberg is gratefully acknowledged and the suggestions and help of Professor Richard Roberts is greatly appreciated.

The author acknowledges the help of Mr. Richard Korastinsky with the electron fractographic work.

Finally, the author gratefully appreciates the financial support of the National Science Foundation under Grant GK 1225.

# Table of Contents

# List of Tables

## List of Figures

## Abstract

The macroscopic and electronmicroscopic crack propagation behavior of 2024-T3 aluminum alloy resulting from the application of a single 50% overload in an otherwise uniform alternating fatigue load is examined. It is observed that the change in the stress intensity factor, K, caused by the peak load at varying crack lengths has a considerable effect on fatigue crack propagation and fracture surface appearance. The overload causes retardation of the crack growth rate, which becomes more pronounced as the peak load stress intensity conditions are increased. At low stress intensity conditions the fracture surface reveals the progress of the crack to be that of striation formation before the overload, a stretch zone or very large striation formed due to the overload and striation formation after the overload. At higher stress intensity conditions the stretch zone is immediately followed by either dimple formation or an abraded region before the resumption of striation formation. Consequently, stable crack extension is found to occur by both a stretching process and by void coalescence. Correlation of macro-growth rate data and micro-growth rate data, as measured by striation spacing, is good.

## Introduction

The growth of a crack due to a simple sinusoidal loading pattern has been studied extensively and laws have been proposed to predict the crack growth in terms of certain significant parameters[1-5]. Most of these crack propagation laws were obtained for a limited amount of data; their validity over a large range of data was questioned by Paris and Erdogan.[6] They concluded that the most consistent agreement with the experimental data was obtained with the fracture mechanics approach, where an approximately fourth power dependence of the stress intensity factor range, $\Delta K$, on the crack growth rate existed over an extensive range of data. Different power relations have been suggested, but the dependence of the stress intensity factor on crack growth has been well established.

Hudson and Hardrath[7] and others[8,9] have noted the effect of changing the stress level on the crack growth of a specimen. If the initial stress level was higher than the second one, the crack propagation at the second level was delayed, but if the first level was lower than the second, the effect of the first stress level on the growth at the second stress level was not noticeable. The delay was attributed to the formation of residual stresses ahead of the crack because of the higher cyclic stresses of the

first stress level. A similar behavior was noticed by Schijve and Broek[8] and by Hardrath and McEvily[9] who also attributed the delay to the residual stress formation ahead of the crack.

Schijve and Broek[9] found that a single overload cycle also resulted in retardation of the crack growth. They found that the retarding effect of the peak load was substantially greater when only a positive peak was applied, as compared to the application of a complete peak load cycle with a negative peak as well. Throop[10] investigated the effect of an overload on the total fatigue life of a specimen and on the crack propagation rate, and concluded that the rate of crack propagation depended on the plastic zone formed during the overload cycle and on the residual zone remaining after the overload had been removed. McMillan and Hertzberg[11] observed that, when applying a complete peak cycle (positive and negative peak), the order in which they were applied, i.e., positive peak first or second, had a pronounced effect on the subsequent crack growth rate. They also found that by increasing the magnitude of the peak load from 75% to 150% of the loading range the fatigue life was increased.

The microscopic appearance of fatigue fracture surfaces has been studied to further our understanding of the fatigue process.[12,13,14] The fracture surface of a fatigued

component reveals many areas containing parallel markings called striations, each representing one cycle of loading. The relationship between these markings and macroscopic crack growth has been the object of considerable work;[12,15,16] there generally is good correlation between the growth rate obtained macroscopically and the growth rate measured from striation data.

McMillan and Hertzberg[11] investigated the effect of the application of a peak load on the electronmicroscopic appearance of the fracture surface and found that the peak load could be identified as a stretch band or large striation between two sets of striations.

The purpose of this investigation was to study the effect of the relative position at which a fixed percentage overload was applied on macroscopic crack extension and on the microscopic appearance of the fracture surface. The effect of the thickness of the specimen at equivalent stress intensity conditions on the crack growth rate and the fracture surface appearance was also investigated.

## Experimental Procedures

### A. Materials

The material investigated was .126" and .094" thick 2024-T3 aluminum alloy.

### B. Specimen Preparation and Testing Procedures

Tensile coupons of the aluminum alloy were tested on a Baldwin Testing Machine to obtain yield stress, tensile stress, % elongation and % reduction in area measurements of the specimens.

Single edge-notched specimens with a starting crack length of 1/2" to 7/8" were used for the fatigue and overload studies. All starting notches were sharpened with a scalpel blade. The configuration of the specimens is shown in Fig. 1. The load cycling was done on an Instron Testing Machine. The loading range for the .126" aluminum alloy specimens was from zero to 1900 lbs. and the loading speed ranged from 16 to 23 cpm.. For the .094" thick specimens the range of loads was from zero to 1400 lbs. and the loading speed varied from 18 to 21 cpm..

The progress of the crack was measured with a Gaertner traveling microscope.

In all cases but one, the specimen was subjected to a 50% overload. The crack length where the peak load was applied was varied to study the material response when the

peak stress intensity factor due to the overload was changed as a result of different starting or base stress intensity conditions. The percent overload, crack length at overload, stress intensity conditions prior to and at the peak stress, are tabulated in Table I and the loading program is schematically shown in Fig. 2.

C. Fractographic Techniques

The surfaces of the specimens were cleaned with an ultrasonic cleaner (DiSontegrator). 5 mil cellulous acetate replicating tape was softened with acetone and applied to the fracture surface. After the tape had been allowed to dry it was removed from the surface and shadowed with C-Pt pellets in the approximate direction of the crack growth; carbon then was deposited normal to the replica surface. After dissolving the replicating tape in acetone and placing the carbon replica on 200 mesh stainless steel grids, it was examined in an RCA EMU-3G electron microscope. Most of the fractographic work was done at a magnification of 8000 X with an accelerating potential of 50 KV.

To obtain microscopic growth rate data over the whole life of a specimen, 2 mm. long replicas were viewed. Striation spacings were measured throughout the entire replica and the average growth rates assumed to occur at the midsection.

## D. Calculations

The stress intensity factor, K, was obtained from the following formula:

$$K = \sigma\sqrt{\pi a} \cdot k(a/b)$$

where k(a/b) is the Gross correction factor for single edge cracks in finite plates, "a" is the crack length, and σ is the stress. Therefore, referring to Fig. 2

$$K_1 = \sigma_1\sqrt{\pi a} \cdot k(a/b)$$

$$K_2 = \sigma_2\sqrt{\pi a} \cdot k(a/b)$$

For the purpose of analysis, the plastic zone size was considered to be a characteristic length of plastically deformed metal associated with the advancing crack tip. The plastic zone sizes were calculated by the following formulas:

$$r_p = \frac{1}{2\pi}\left(\frac{K_2}{\sigma_{YS}}\right)^2 \qquad \text{plane stress}$$

$$r_p = \frac{1}{6\pi}\left(\frac{K_2}{\sigma_{YS}}\right)^2 \qquad \text{plane strain}$$

$$w = \frac{1}{2\pi}\left(\frac{K_1}{2\sigma_{YS}}\right)^2 \qquad \text{fatigue}$$

and were tabulated in Table II.

## Results

### A. Tensile Behavior

The tensile behavior of the .126" aluminum alloy was investigated. Some scatter was found in the test results as can be seen on Table III. The per cent elongation varied from 12 to 18.5%. The yield stress varied from 50,400 to 53,900 psi. and the tensile strength from 70,200 to 72,700 psi. Reductions in area varied from 5.4 to 19.1%.

### B. Effect of Overloads on Fatigue Crack Propagation

In all specimens tested a retardation in the crack growth rate after the application of the peak load was observed. This effect was more pronounced in some cases than in others, but the general form of the crack length, a, versus the number of cycles, N, was always the same. The immediate effect of the peak load was a deceleration in the crack growth rate, which did not, however, achieve its minimum value immediately after the peak load. Instead the crack decelerated and reached its lowest value some distance beyond the point of application of the overload. After this point the crack growth rate increased till the specimen broke. A typical crack length versus number of cycles curve is shown in Fig. 3. The retarding effect is perhaps more evident in Fig. 4, where the growth rate is plotted against the crack length. The shape of this latter curve

varied with the stress intensity conditions; at higher crack lengths where the peak load was applied, the retarding effect became more pronounced and a larger distance of crack extension was necessary for the crack to reestablish the growth rate it had before the application of the peak load.

The effect of the peak load on the overall fatigue life of the specimen was one of retardation in all specimens investigated. Because of the scatter, however, few quantitative conclusions can be made as to the effect of the crack length at application on the total fatigue life of the specimen.

C. Fatigue Fracture Surface Appearance

1. Macroscopic

When an overload was applied to a specimen the surface of the specimen showed some plastic deformation in the form of localized necking. Two short bands were formed at the crack tip at an angle of approximately 45° to the crack front. Fig. 5 shows a specimen where these bands can be seen quite readily. A number of peak loads were applied and in each case plastic deformation occurred. The higher the crack length at application of the peak load, and, therefore, the higher the stress intensity conditions, the more pronounced the plastic deformation became.

The application of the peak loads produced also

noticeable deformation bands on the fracture surface. Fig. 6 shows these dark bands in a specimen subjected to multiple peak loads. The width of the bands increased with increasing peak stress intensity conditions. For example, in specimens 1M14 and 1M16 (lowest crack lengths at application of the peak load) these bands were hardly discernible, while specimen 1J22 had a band .02" wide.

2. Microscopic.

It was found that the appearance of the fracture surface depended not only on the stress intensity conditions at which the peak load was applied, but varied to a considerable extent with the local crystallographic and metallurgical conditions along the crack front at the time of the peak load application. For example, the presence of broken particles before and immediately after the overload region affected the fracture surface appearance. Consequently, a variety of surface appearances were found within localized areas of the fracture surface.

Table IV summarizes the appearances of the fracture surface before and after the peak loads. Some general trends can be found regarding the effect of the peak load on the fracture surface appearance of a specimen:

a. The general appearance of the fracture surface at low peak stress intensity conditions revealed striations followed by a stretch region (which can be thought of as a

big striation) followed by striations. The stretch region was associated with the peak loading cycle. In addition to this sequence of morphological features on the fracture surface other details were observed; elongated dimples due to void coalescence and abrasion markings resulting from extensive rubbing together of the crack surfaces could be found following the stretch zone over a portion of the fracture surface.

b. With increasing stress intensity conditions, the larger stretch regions were followed increasingly more often by dimpled regions rather than by large packets of striations.

c. It was not unusual to find packets of striations or dimples within the abraded region close to the peak load. This seems to indicate that in the abraded region striations and dimples had originally formed but were subsequently rubbed out.

d. The width of the stretch zone increased as the peak stress intensity conditions increased, till a terminal value of stretch zone size of approximately $2.5 \times 10^{-4}$ in. was reached.

e. After the peak load the size of the striation spacings decreased to a minimum value and then increased in a more normal fashion. Though scatter in the striation measurements was observed, the above trend was definitely

established.

f. The thinner specimens tested showed a greater tendency to have a striations-stretch zone-striations pattern at the same stress intensity conditions than did the thicker ones.

D. Macroscopic vs. Microscopic Behavior

In general it was observed microscopically and macroscopically that the crack growth immediately after the peak load decelerated to a minimum value. After this point the rate increased continuously till the specimen broke. For some specimens microscopic growth rates were determined from striation data throughout the life of the specimen (Fig. 4). Correlation between the growth rates obtained macroscopically and microscopically throughout the life of the specimen were good. At rather high growth rates striation spacing data yielded lower growth rates than those found macroscopically (Fig. 4). The erratic data obtained microscopically makes it necessary for many readings to be taken, as single values can be extremely misleading.

## Discussion of Results

### A. Tensile Behavior

The ASM Metals Handbook[17] gives the following typical mechanical properties for 2024-T3 aluminum alloy:

Yield strength..... 50,000 psi.

Tensile strength..... 70,000 psi.

Elongation..... 18%

Referring to Table III one finds some variation in the mechanical properties of the specimens tested, even though they were all obtained from the same sheet. The elongations in the specimens tested were generally below the handbook value, while the yield strength was somewhat higher than the quoted value. The tensile strength was very close to the one found in the handbook. Since ductility has a definite effect on the growth rate of a specimen, the diversity in elongation data found in the test material would be expected to result in specimen to specimen variations in crack propagation rates. Since the 50% overload cycle did not result in significant crack propagation delay, some of the overload data tend to be obscured by metallurgical variations.

### B. Effect of Overloads on Fatigue Crack Propagation

A clear, quantitative relationship between crack

tip stress intensity conditions at the peak load and its retarding effect upon fatigue life could not be found, since the 50% peak load did not produce large delays. Consequently, these delays were sometimes overshadowed by the scatter found in the normal fatigue growth data. However, based on the observed behavior and theoretical considerations, a general relationship may be suggested.

Associated with a fluctuating fatigue load is a plastically yielded zone ahead of the crack of approximate size given by:

$$W = \Delta K^2/8\pi\sigma_{YP}{}^2$$

in which residual tensile or compressive stresses are created with every excursion of the load. When an overload is applied the higher stress intensity conditions create a larger plastic zone in which a more severe residual compressive stress field exists; this results in retardation of the crack growth rate when the loading returns to a lower constant fluctuating load. The retarding effect becomes more severe as the peak load stress intensity conditions are increased.

However, when the plastic zone size becomes large with respect to the dimensions of the specimen and the volume of the elastic material surrounding the plastic enclave becomes small, the constraining effect of the elastic material on the plastic zone diminishes. Consequently the resid-

ual compressive stresses become smaller.

As a result, the retarding effect of an overload is governed by both the peak stress intensity conditions and the constraining effect of the elastic material on the plastically yielded zone. It can therefore be expected that for a given material and specimen geometry, a given peak load stress intensity condition would result in maximum retardation. Conversely, it may also be expected that a given peak load stress intensity condition would result in immediate fracture of the specimen. This proposed behavior is illustrated in Fig. 7.

The general effect of an overload on the propagation of a crack is shown in Fig. 4, a plot of crack length versus crack growth rate. As the peak stress intensity conditions increased, i.e. the crack length at application of the peak load was increased, the dip in the plot became deeper and wider, indicating greater crack extension delay. The decrease in retardation suggested in Fig. 7 was not observed in this investigation because the plastic zone size was never large compared to the dimensions of the specimen.

An approximate one-to-one correlation was found between the size of the plane strain plastic zone size (see Table II) and the distance beyond the peak load at which the crack reached a minimum growth rate. The existence of this condition is not well understood in view of the ap-

proximations associated with the size of the plastic zone. Nevertheless, the correlation is consistent with the tendency for maximum triaxiality, and hence plastic constraint, to occur near the boundary of the plastic zone.

C. Fatigue Fracture Surface Appearance

1. Macroscopic

Application of a peak load results in plastic deformation, which becomes more severe with increasing stress intensity conditions. Any macroscopic changes noted as a result of the application of the overload became, as expected, more pronounced at the higher peak load stress intensity conditions.

In the specimens where the crack length was relatively short when the overload was applied, such as 1M14 and 1M16, the existence of a peak load was considerably less apparent than in those specimens where the crack length was longer. In both 1M14 and 1M16 a narrow shiny band was observed where the overload was applied, while at those specimens where the peak stress intensity conditions were more severe a dark band was formed, increasing in size as the overload was applied at higher crack lengths.

A similar phenomenon was observed regarding the exterior appearance of the specimen at the crack tip when the overload was applied. In 1M14 and 1M16 there was little plastic deformation as evidenced by localized surface neck-

ing, while this localized yielding became more evident as the crack length at peak load application increased (Fig.5).

2. Microscopic

The existence of an overload was identified microscopically by a stretch band considerably larger than the striations preceding it. The stretch zone increased in size as the peak load stress intensity conditions became more severe, till it reached a limiting value of about $2.5 \times 10^{-4}$ in.. At higher stress intensity conditions, crack extension due to the peak load was accomplished by the stretching process plus microvoid coalescence. This observation is consistent with the suggestion of McClintock and Pelloux[18]; at low stress intensity levels, with a sharp crack radius, crack extension should occur by a sliding off process (i.e. stretching region) while at high stress intensity conditions with blunt notches the crack would advance by microvoid coalescence. The peak loads at higher stress intensity conditions in this investigation evidently revealed this fracture mechanism transition when the crack tip became sufficiently blunted due to the extensive stretching process.

At low peak load stress intensity conditions the stretch zone was followed by striations, since sliding did not change to void formation (Figs. 8 & 9). At higher peak load stress intensity conditions growth by void coalescence (dimples) became more prevalent (Figs. 10 & 11). In addi-

tion, at both low and high stress intensity conditions, there sometimes was considerable rubbing of the crack surfaces resulting in a rather featureless abraded appearance (Figs. 12 & 13).

Referring to Tables I and IV it is observed that a striations-stretch band-striations pattern exists at higher stress intensity conditions for the .094" specimens than for the .126" ones. Because there is less elastic constraint in the thinner specimens, lower residual compressive stresses are formed ahead of the crack and therefore less retardation should be expected for these specimens. However, no discernible differences in delays were observed between both sets of specimens at equal stress intensity conditions; this is believed to be due to the scatter and local variations in metallurgical conditions at the peak load crack position. Broken particles, for example, altered the local stress intensity conditions (notice the small striations preceding the overload in Fig. 14). In this example, striations were found to follow the stretch zone in a specimen where this behavior was seldom observed. In this particular case, the smaller striations preceding the overload reflected a lower local stress intensity condition and a sharper crack tip radius. The subsequent peak load did not produce sufficient blunting to cause the formation of microvoids, but rather led only to the formation

of a stretch zone followed by striations. These latter striations were larger than those occurring before the peak load since the crack length in this local region was now larger along with the stress intensity conditions.

It was often observed that in the abraded region following the overload small packets of striations could be found. In Figs. 15 & 16 striations and abrasion can be seen following the stretch band. This indicates that there was considerable rubbing of the surfaces which destroyed most of the striations, but actually there still were striations being formed and the crack continued to grow. Because striations continued to be formed it can be concluded that the crack is retarded and not stopped (the small size of the striations after the stretch zone reflects the slower growth rate). Similarly, regions of dimples were found within the abraded region (Fig. 17) of specimens tested at high stress intensity levels. It can also be concluded that the advance due to the overload is a combination of stretching and dimple formation, and that abrasion does not necessarily imply much delay, but only indicates that there has been considerable rubbing of the surfaces.

## Conclusions

The following conclusions can be drawn from this study:

1. In all cases the 50% overload caused retardation in the crack growth rate. However, the 50% peak load was not sufficiently severe to overshadow the scatter of normal fatigue data and yield meaningful quantitative information regarding the effect of the position at which the overload was applied on the growth rate and fatigue life.

2. The minimum crack extension rate was reached at a distance approximately equal to the plane strain plastic zone size beyond the point of application of the peak load.

3. At low peak load stress intensity conditions the microscopic fracture surface appearance due to the overload was one of striations-stretch zone-striations.

4. At high peak load stress intensity conditions, because of growth due to void coalescence, dimples followed the stretch zone formed during the overload cycle.

5. At both high and low peak load stress intensity conditions regions of abrasion followed the stretch band in some areas, because of rubbing of the fracture surfaces.

6. Under similar stress intensity conditions the .094" specimens showed a greater propensity towards a striations-stretch zone-striations pattern than the .126" specimens. This was believed to be due to less elastic constraint in the thinner specimens.

7. There was strong correlation between the observed macroscopic growth rate and the growth rate obtained microscopically from striation data.

## Table I

## STRESS INTENSITY CONDITIONS IMMEDIATELY PRECEDING AND DURING OVERLOAD CYCLE

| Specimen | Thickness (in) | Per Cent Overload (%) | C.L. (in) | $\sigma$ (psi) | $K_1$ (psi$\sqrt{in}$) | $K_2$ (psi$\sqrt{in}$) |
|---|---|---|---|---|---|---|
| 1M14 | .126 | 50 | .702 | 4930 | 11,160 | 16,740 |
| 1M16 | .126 | 50 | .783 | 4930 | 12,700 | 19,050 |
| 1M10 | .126 | 50 | .792 | 5070 | 13,150 | 19,730 |
| 1M2 | .126 | 50 | 1.005 | 4990 | 15,700 | 23,550 |
| 1J12 | .126 | 50 | 1.048 | 4990 | 16,700 | 25,050 |
| 2C6 | .094 | 50 | 1.048 | 5100 | 17,050 | 25,580 |
| 1J14 | .126 | 50 | 1.100 | 4990 | 17,400 | 26,100 |
| 2C8 | .094 | 50 | 1.092 | 5100 | 17,650 | 26,480 |
| 2C10 | .094 | 50 | 1.100 | 5100 | 17,800 | 26,650 |
| 1J16 | .126 | 50 | 1.161 | 4990 | 18,300 | 27,450 |
| 1J20 | .126 | 50 | 1.192 | 4990 | 19,000 | 28,500 |
| 1J22 | .126 | 50 | 1.240 | 4990 | 19,450 | 29,180 |
| 2C12 | .094 | 100 | 1.100 | 5100 | 17,800 | 35,600 |

C.L.: Crack Length at Overload Application

$\sigma$ : stress range before peak load application

$K_1$ : stress intensity factor range immediately preceding overload

$K_2$ : stress intensity factor range for overload cycle

## Table II

## CALCULATED PLASTIC ZONE SIZES

| Specimen | Plane Stress (in) | Plane Strain (in) | Fatigue (in) |
|---|---|---|---|
| 1M14 | .0179 | .0037 | .0019 |
| 1M16 | .0210 | .0069 | .0022 |
| 1M10 | .0229 | .0075 | .0025 |
| 1M2 | .0314 | .0104 | .0035 |
| 1J12 | .0371 | .0123 | .0041 |
| 2C6 | .0380 | .0129 | .0042 |
| 1J14 | .0389 | .0130 | .0044 |
| 2C8 | .0408 | .0135 | .0047 |
| 2C10 | .0422 | .0138 | .0048 |
| 1J16 | .0440 | .0148 | .0050 |
| 1J20 | .0481 | .0161 | .0053 |
| 1J22 | .0499 | .0167 | .0057 |
| 2C12 | .0741 | .0248 | .0081 |

## Table III

## TENSILE BEHAVIOR OF 2024-T3 ALUMINUM ALLOY

| Specimen | Per Cent Elongation (%) | Per Cent Reduction in Area (%) | .2% Yield Stress (psi) | Tensile Strength (psi) |
|---|---|---|---|---|
| 1M1 | 12.0 | 5.6 | 50,400 | 70,200 |
| 1M3 | 12.7 | 5.4 | 53,300 | 71,800 |
| 1M5 | 12.5 | 6.9 | 53,200 | 71,900 |
| 1M7 | 13.0 | 6.4 | 51,700 | 72,000 |
| 1M9 | 17.5 | 18.7 | 51,200 | 72,000 |
| 1M11 | 13.5 | 8.2 | 51,500 | 71,000 |
| 1J11 | 16.5 | 12.0 | 53,600 | 72,000 |
| 1J13 | 12.5 | 8.0 | 53,400 | 71,400 |
| 1J15 | 18.0 | 19.1 | 52,000 | 71,000 |
| 1J17 | 18.5 | 17.5 | 53,800 | 72,300 |
| 1J19 | 16.0 | 10.1 | 53,900 | 72,700 |
| 1J21 | 17.0 | 9.8 | 53,300 | 72,400 |

## Table IV

## ELECTRONFRACTOGRAPHIC APPEARANCE RESULTING FROM OVERLOAD CYCLE

| Specimen | Crack Growth Rate Before Peak Load (in/cycle$\times10^{-5}$) | Size of the Stretch Zone Range/Average ($\times10^{-4}$in) | Appearance Immediately After the Stretch Zone (% of Surface) | | |
|---|---|---|---|---|---|
| | | | Str. | D. | Abr. |
| 1M14 | 1.02 | .375-1.25/.625 | 50 | 10 | 40 |
| 1M16 | 1.30 | .500-1.37/1.10 | 50 | 10 | 40 |
| 1M10 | 2.36 | 1.12-1.37/1.25 | 0 | 0 | 100 |
| 1M2 | 2.80 | 1.10-2.10/1.87 | <5 | 30 | 70 |
| 1J12 | 2.52 | 1.00-1.50/1.30 | 0 | 50 | 50 |
| 2C6 | 2.36 | .90-1.75/1.50 | 40 | 10 | 50 |
| 1J14 | 2.52 | 1.00-1.50/1.40 | 0 | 50 | 50 |
| 2C8 | 2.52 | 1.40-1.80/1.60 | 30 | 20 | 50 |
| 2C10 | 2.52 | 1.30-2.50/1.70 | <5 | 30 | 70 |
| 1J16 | 2.80 | 1.00-1.75/1.20 | 0 | 70 | |
| 1J20 | 3.12 | 1.30-2.10/1.70 | 0 | 50 | 50 |
| 2C12 | 2.48 | 1.30-2.30/1.70 | 0 | 70 | 30 |

Str. : Striations

D. : Dimples

Abr. : Abrasions

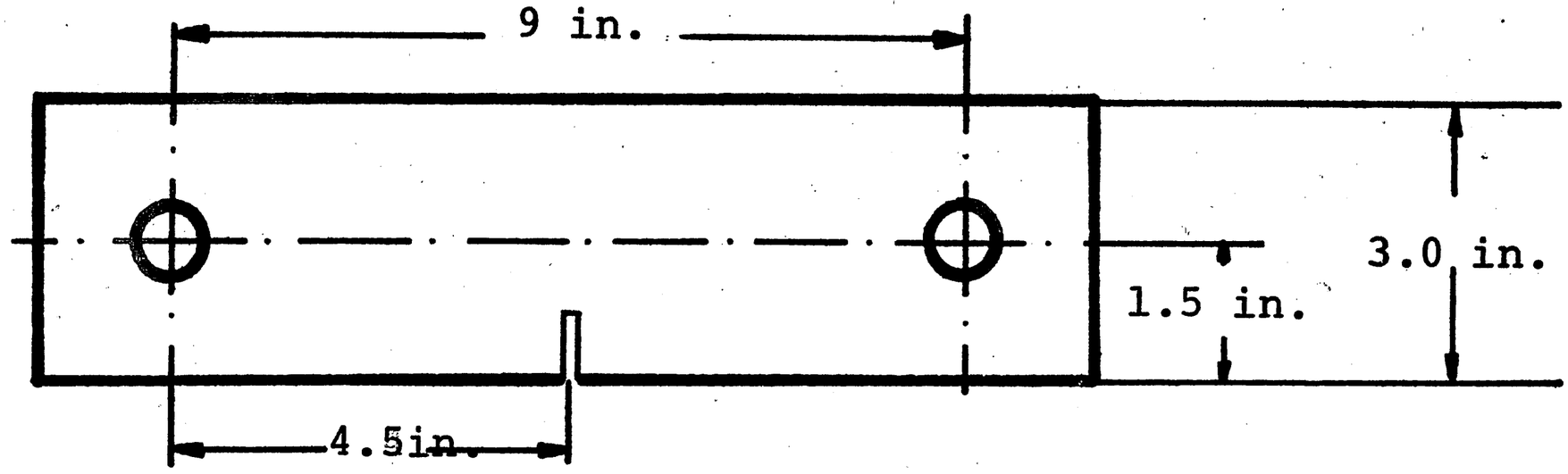


Fig. 1. Configuration of Single Edge-Notch Test Specimen.

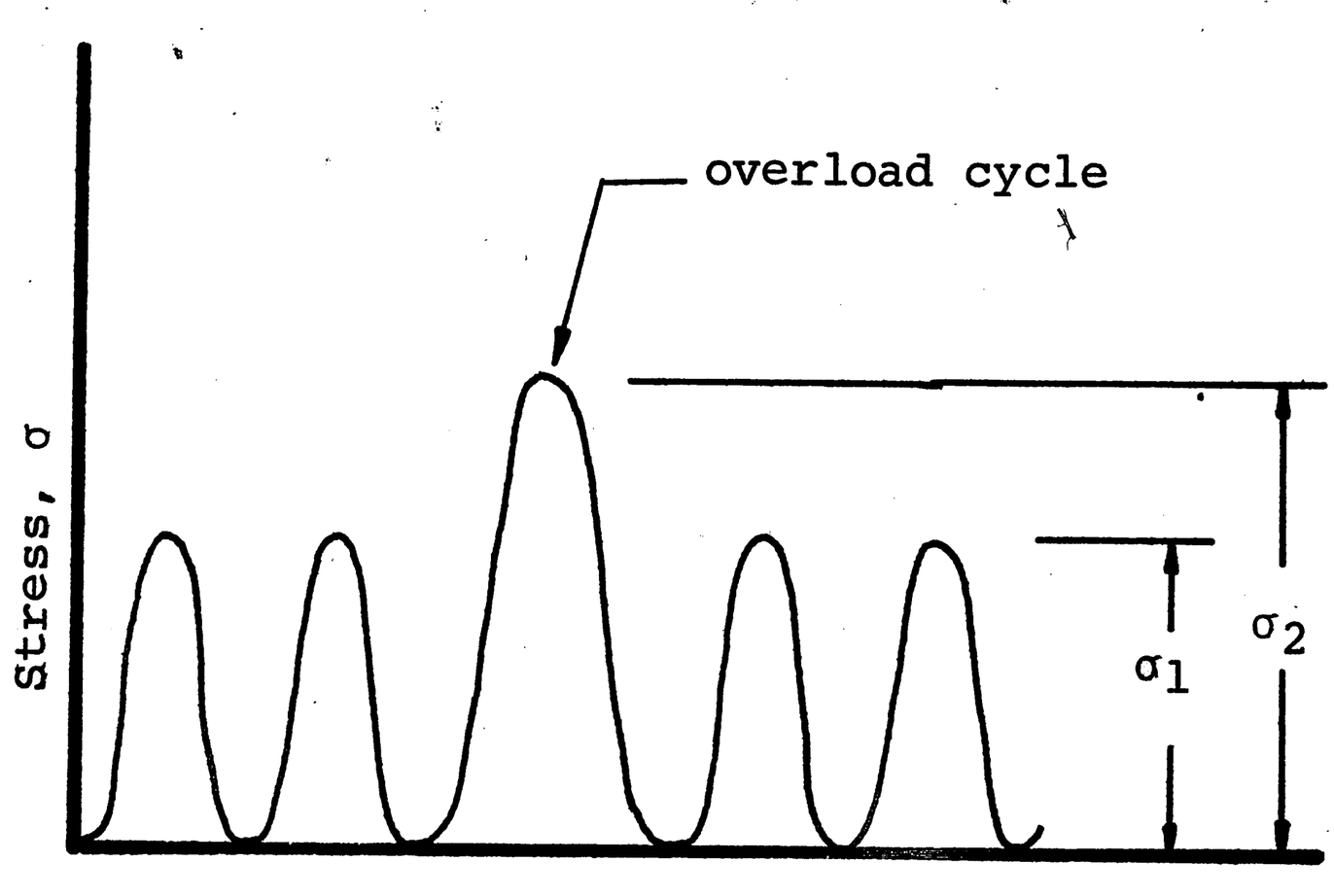


Fig. 2. Schematic Diagram of Loading Sequence Applied to Specimens

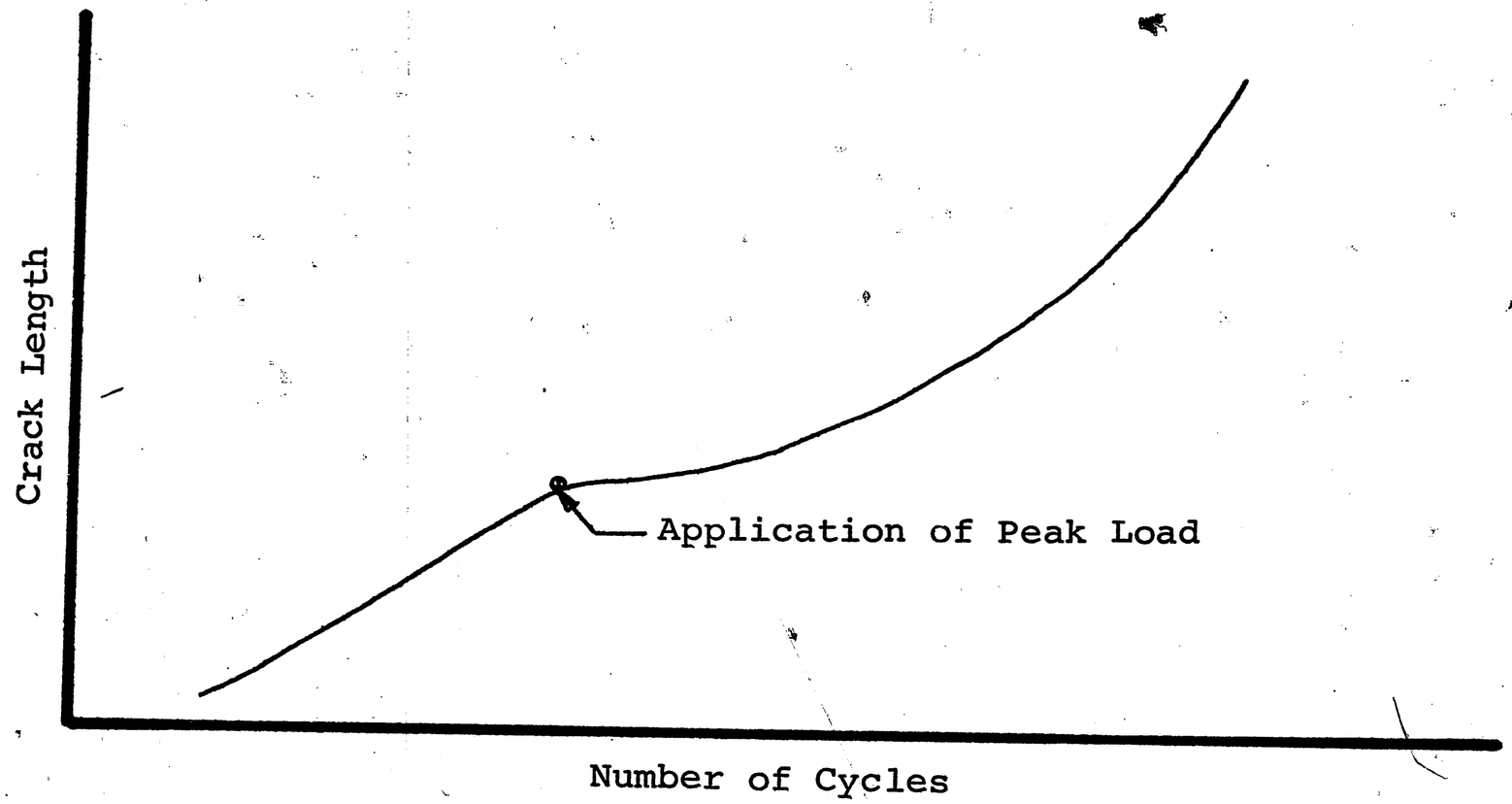


Fig. 3. Plot of Crack Length Versus Number of Loading Cycles for Specimens Subjected to a Peak Load.

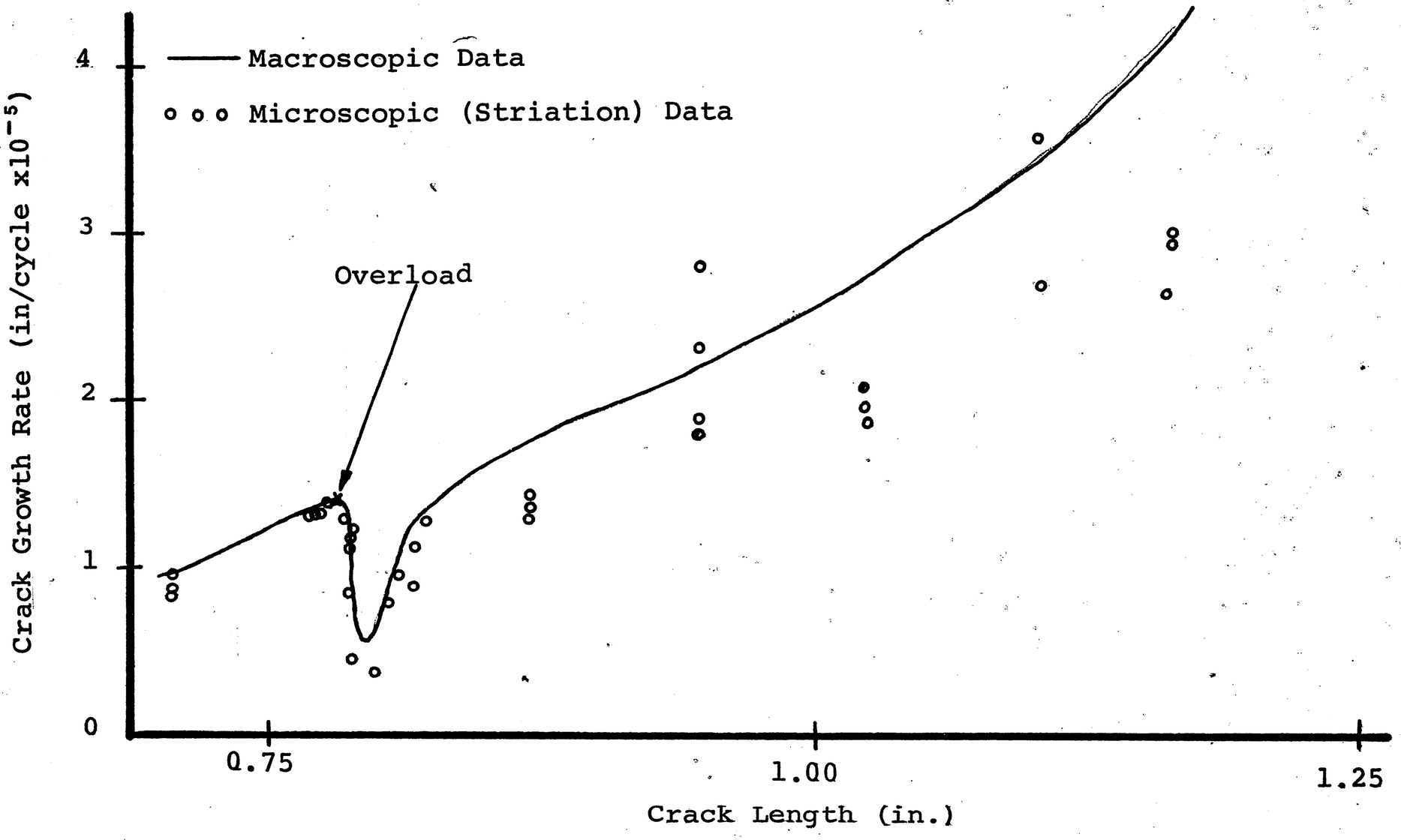


Fig. 4. Plot of Crack Growth Rate Versus Crack Length for a Specimen Subjected to a Peak Load (Macroscopic and Microscopic Data) (Specimen 1M16).

Fig. 5. Photograph of a Specimen Subjected to Several Overloads, Showing the Bands Formed Because of the Localized Necking.

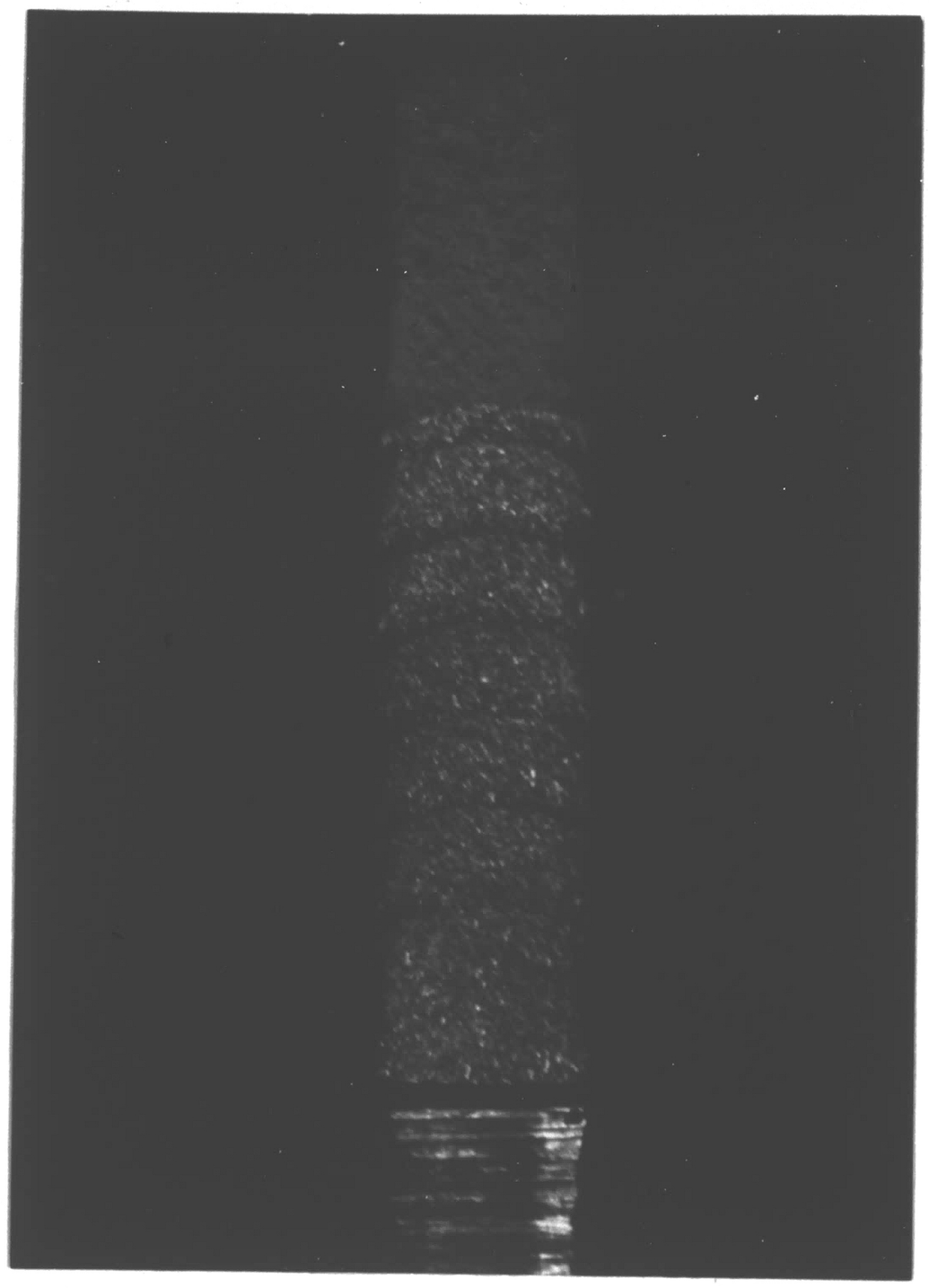

Fig. 6. Photograph of the Fracture Surface of a Specimen Subjected to a Number of Overloads, Showing the Dark Bands Formed as a Result of the Overloads

$a^\circ$ = Crack Length at Application of the Peak Load
$W$ = Width of Specimen
$N_F^\circ$ = Cycles to Fracture With No Overload

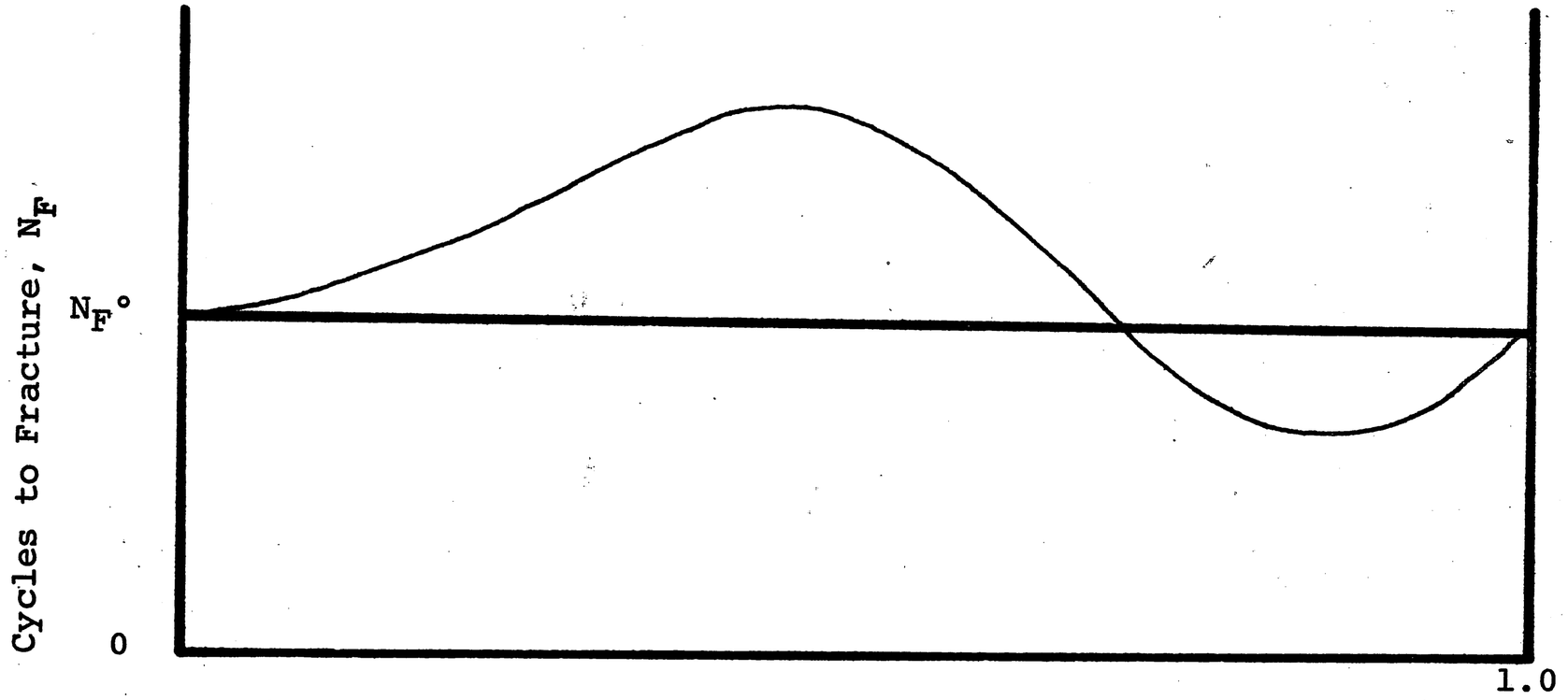


Fig. 7. Proposed Effect of the Position of Application of the Peak Load on the Total Fatigue Life of a Specimen


Fig. 8. Electron Fractograph Showing Effect of an Overload in Low Peak Load Stress Intensity Conditions: Striation (A)-Stretch Band (B)-Striation (C) Pattern. Arrow Indicates Direction of Crack Propagation. (Specimen 1M16), 8000 X.

Fig. 9. Electron Fractograph Showing Well Defined Stretch Band (B) Between Two Sets of Striations (A & C) Resulting from the Application of a Peak Load at Relatively Low Stress Intensity Conditions. Arrow Indicates Direction of Crack Propagation. (Specimen 1M16), 8000 X.

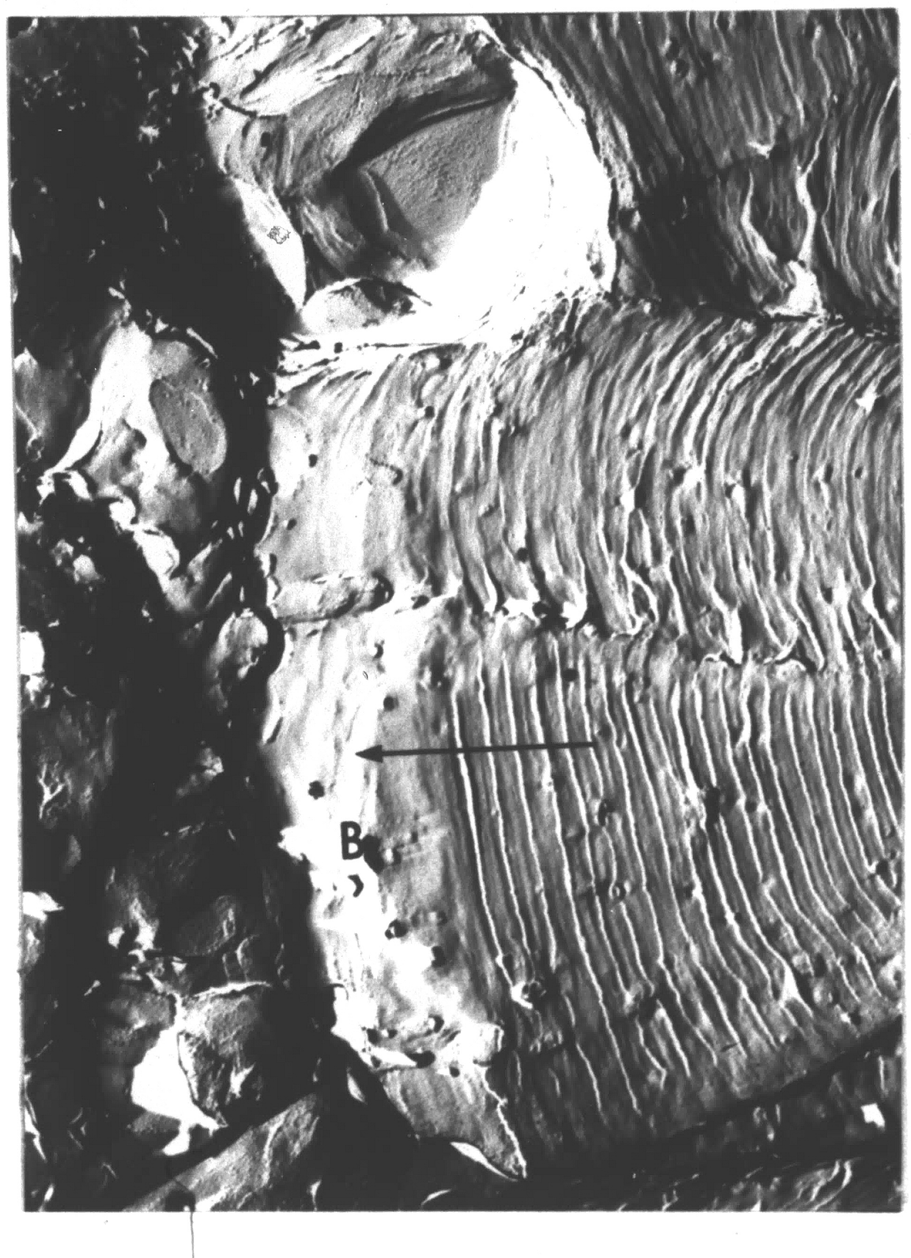


Fig. 10. Electron Fractograph Showing Dimple Formation (A) Because of Growth by Void Coalescence Following the Stretch Zone Resulting from the Application of the Peak Load (B). Arrow Indicates Direction of Crack Propagation. (Specimen 1M14), 8000 X.

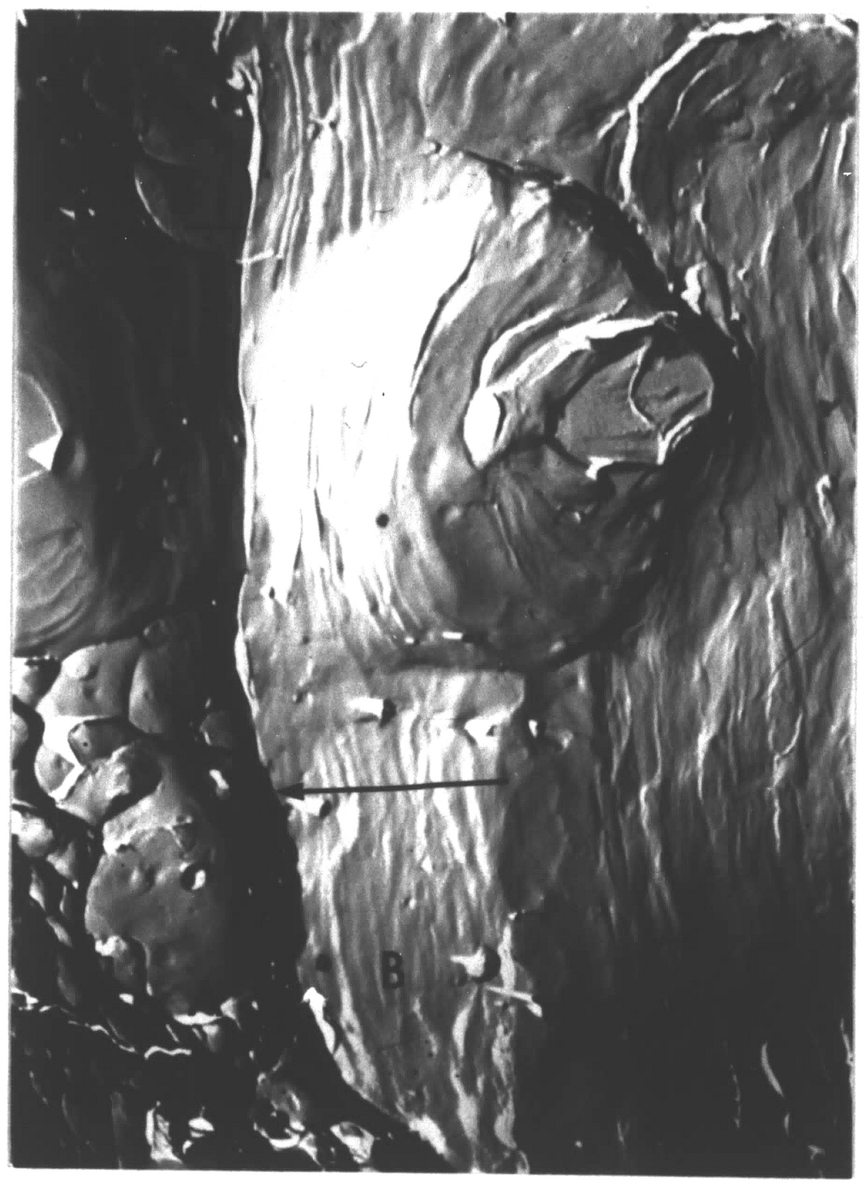


Fig. 11. Electron Fractograph Showing Dimple Formation (A) Following Stretch Zone (B). Arrow Indicates Direction of Crack Propagation. (Specimen 2C10), 8000 X.

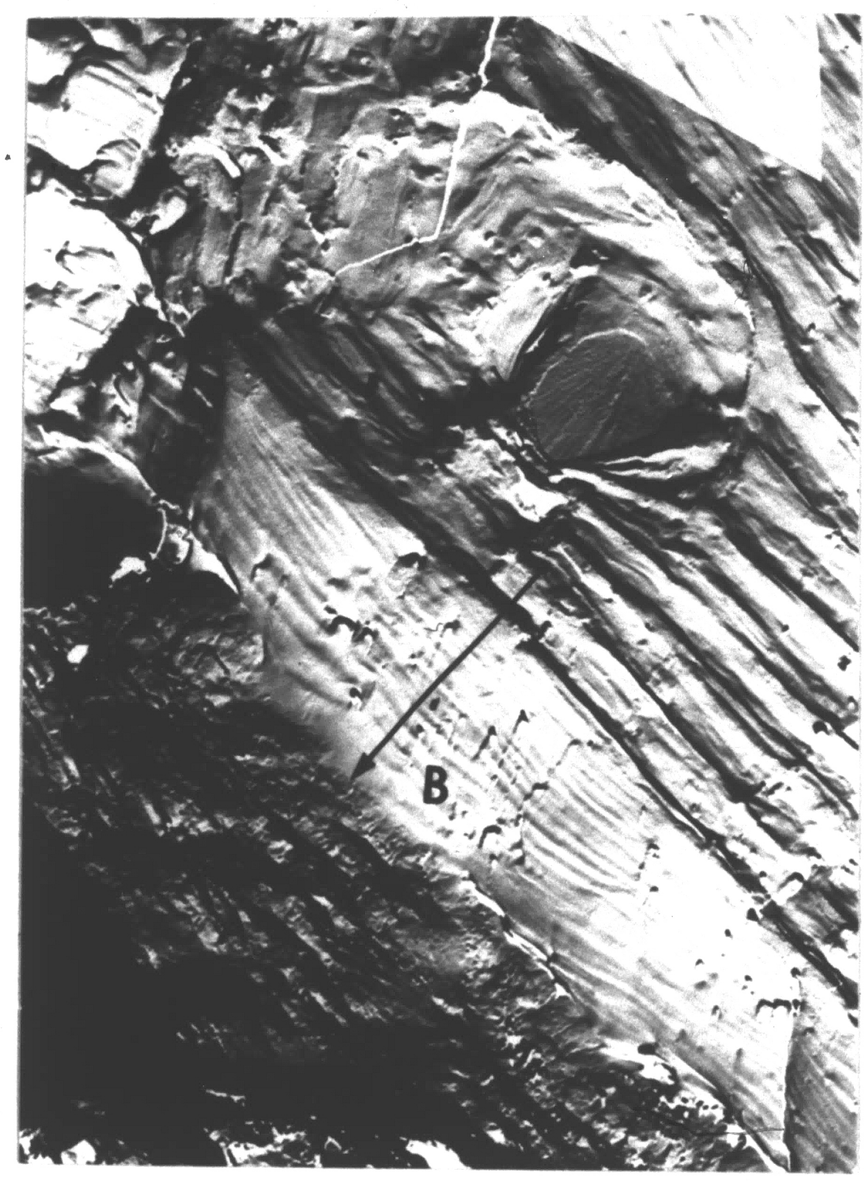


Fig. 12. Electron Fractograph Showing Abraded Region (A) Following Stretch Band (B). Arrow Indicates Direction of Crack Propagation. (Specimen 1J14), 8000 X.

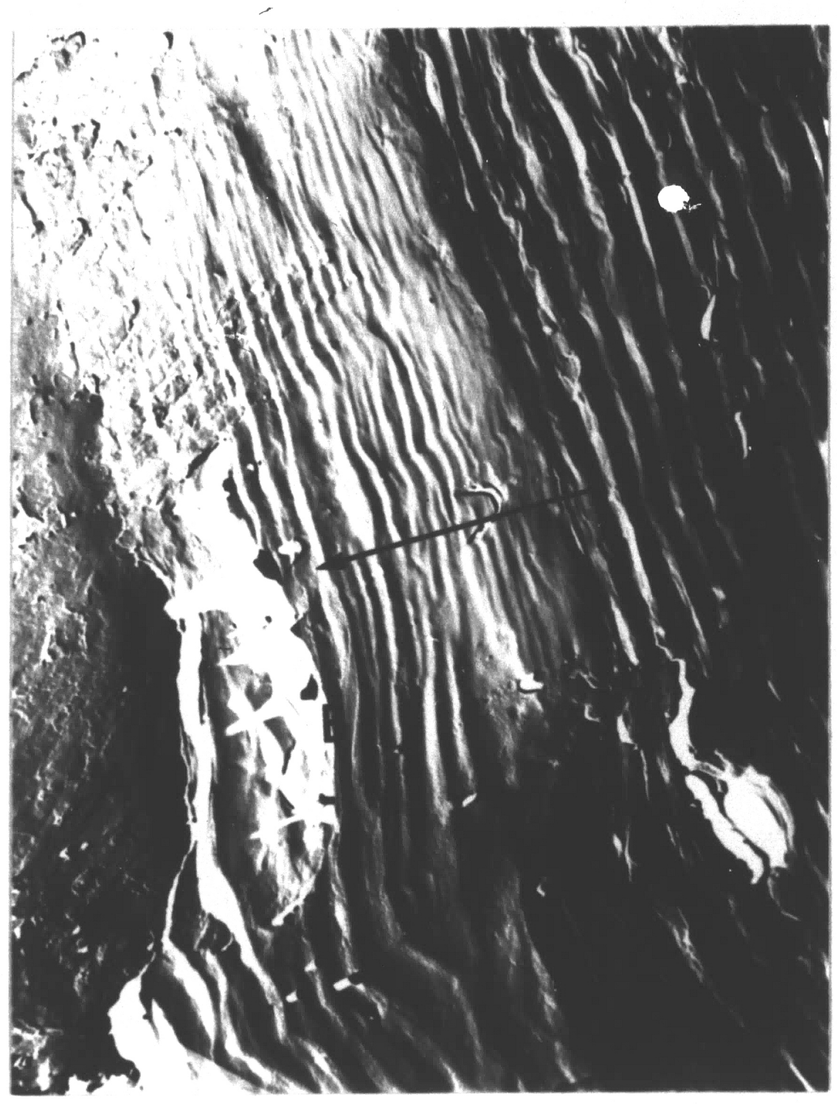

Fig. 13. Electron Fractograph Showing Abraded Region (A) Following Stretch Band (B) at Relatively High Peak Load Stress Intensity Conditions. Arrow Indicates Direction of Crack Propagation. (Specimen 2C8), 8000 X.


Fig. 14. Electron Fractograph of Overload Region. The Broken Particles (A) Preceding the Overload Altered the Local Stress Intensity Conditions and Striation Formation (B) Followed the Stretch Zone (C). Arrow Indicates Direction of Crack Propagation. (Specimen 1M2), 10,000 X.

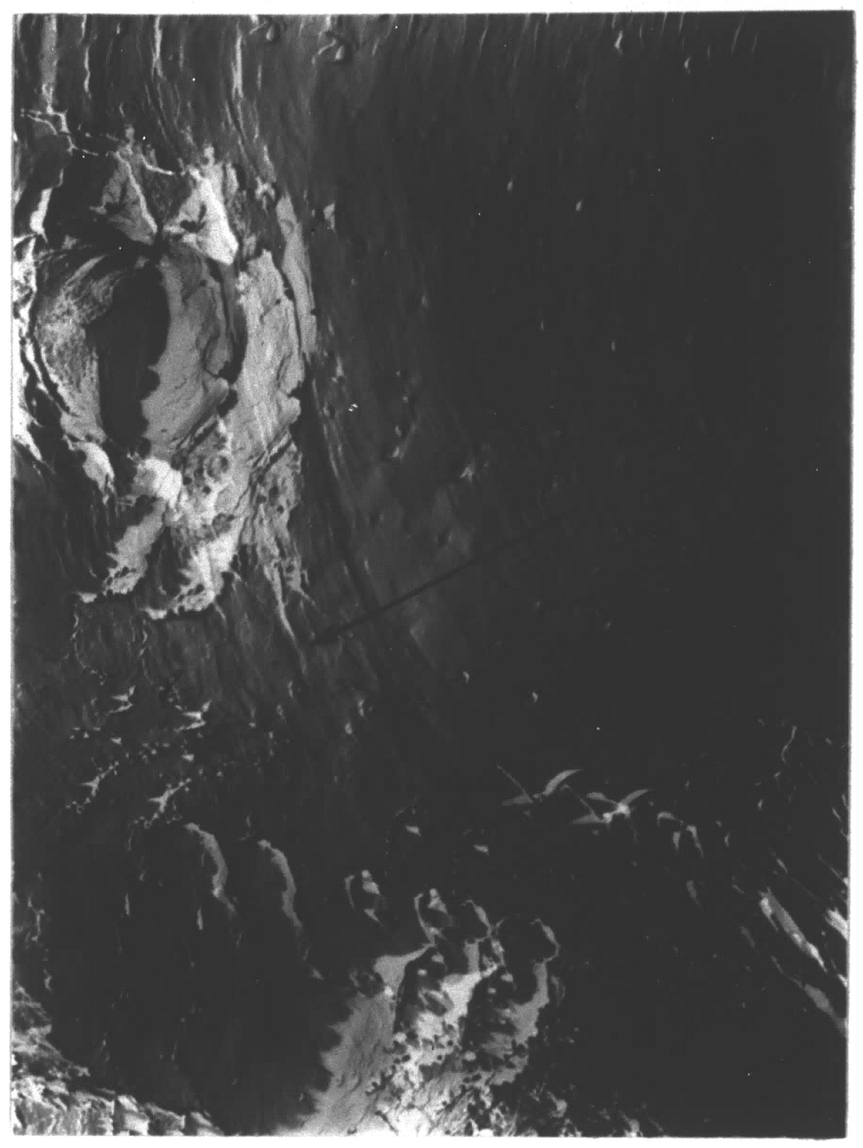

Fig. 15. Electron Fractograph Showing Striations (A) in Abraded Region Following Stretch Zone. Arrow Indicates Direction of Crack Propagation. (Specimen 1M14), 8000 X.

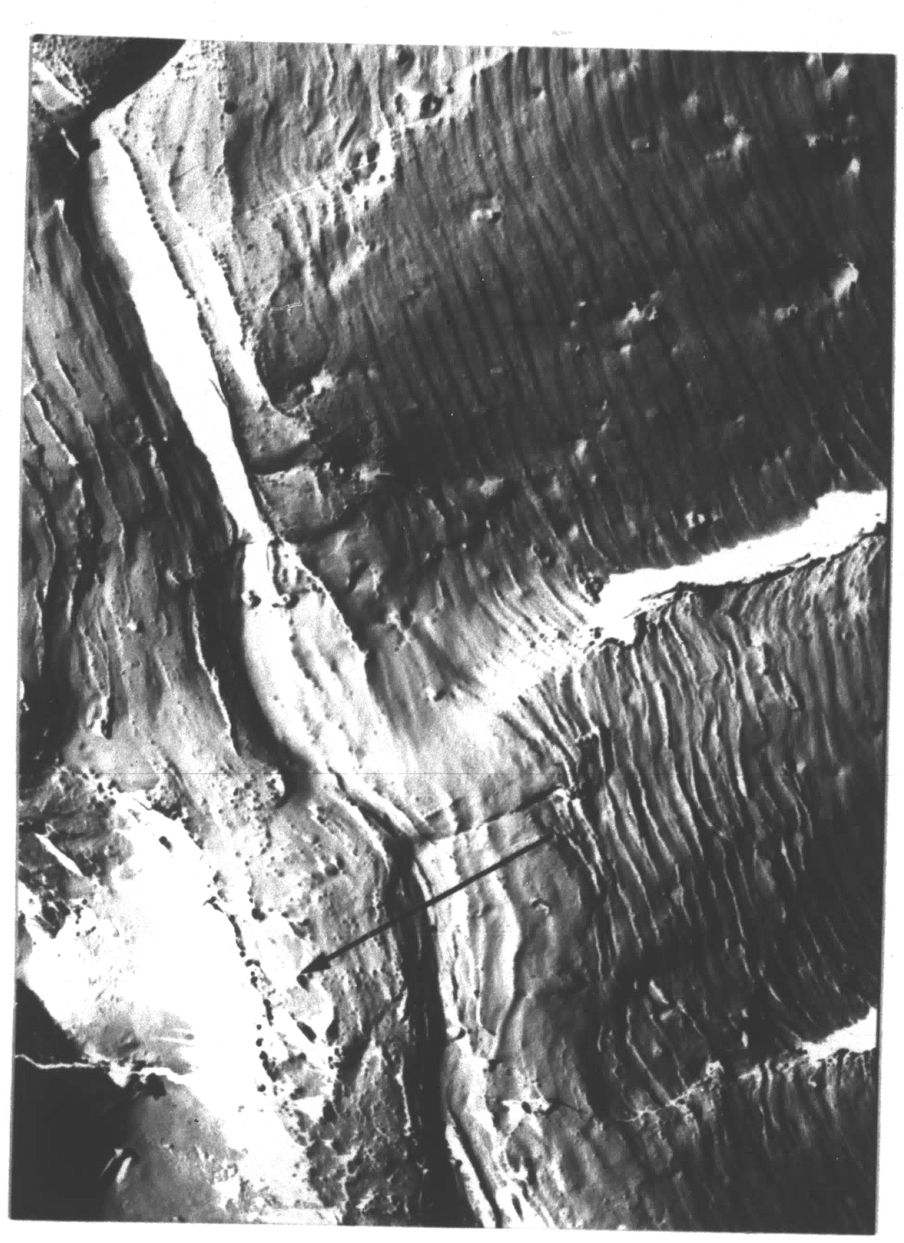

Fig. 16. Electron Fractograph Showing Striations in Abraded Region Following the Stretch Band. Arrow Indicates Direction of Crack Propagation. (Specimen 1M14), 8000 X.

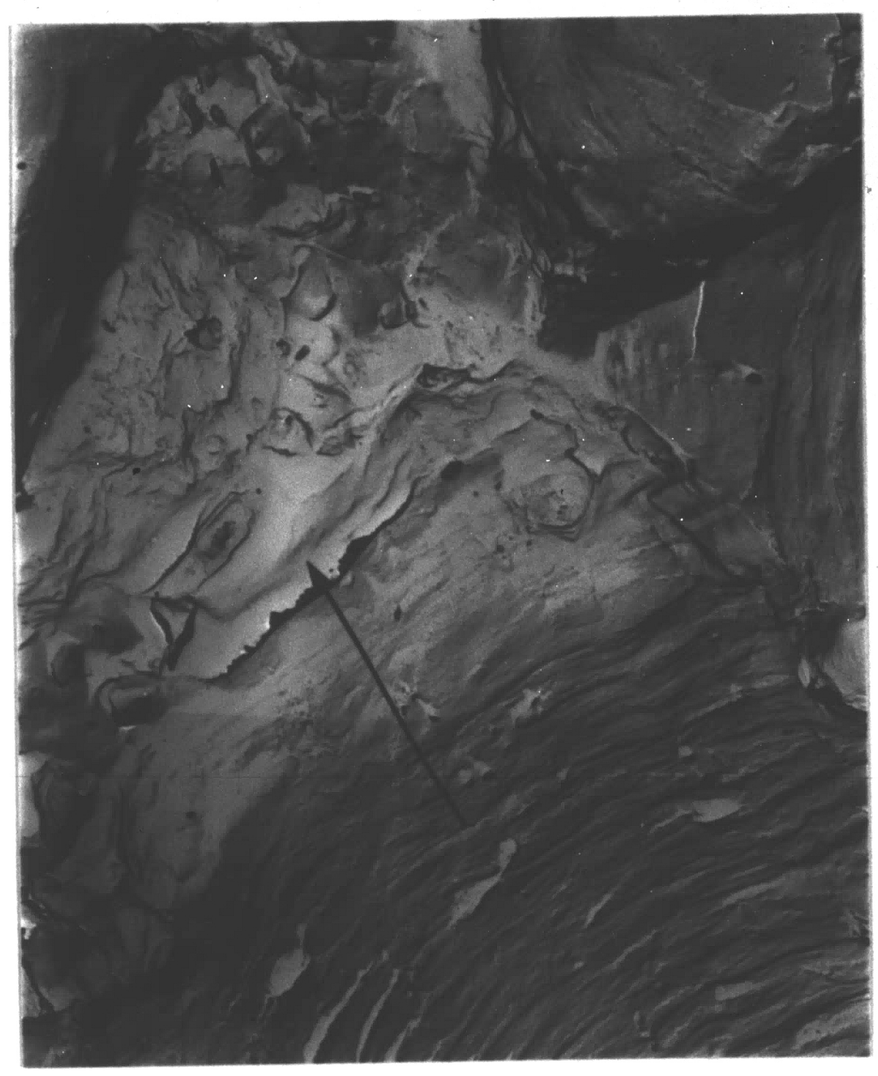

Fig. 17. Electron Fractograph Showing Dimples in Abraded Region Following the Peak Load. Arrow Indicates Direction of Crack Propagation. (Specimen 1M16), 8000 X.

## Bibliography


1. Head, A.K., "The Growth of Fatigue Cracks," The Philosophical Magazine, vol. 44, series 7, (1953), p. 925.

2. Frost, N.E. and Dugdale, D.S., "The Propagation of Fatigue Cracks in Sheet Specimens," Journal of the Mechanics and Physics of Solids, vol. 6, no. 2, (1958), p. 92.

3. Liu, H.W., "Crack Propagation in Thin Metal Sheets Under Repeated Loading," The Journal of Basic Engineering, vol. 83, series D, no. 1, (1961), p. 23.

4. Paris, P.C., Gomez, M.P., and Anderson, W.E., "A Rational Analytic Theory of Fatigue," The Trend in Engineering, vol. 13, no. 1, (1961), p. 9.

5. Liu, H.W., "Fatigue Crack Propagation and the Stresses and Strains in the Vicinity of a Crack," Applied Materials Research, vol. 3, no. 4, (1964), p. 229.

6. Paris, P.C., and Erdogan, F., "A Critical Analysis of Crack Propagation Laws," The Journal of Basic Engineering Trans. ASME, series D, vol. 85, no. 4, (1963), p. 528.

7. Hudson, C.M., and Hardrath, H.F., "Effects of Changing Stress Amplitude on the Rate of Fatigue Crack Propagation in Two Aluminum Alloys," N.A.S.A. Technical Note D-960, (1961).

8. Schijve, J., and Broek, D., "The Results of a Test Programme Based on a Gust Spectrum with Variable Amplitude Loading," Aircraft Engineering, vol. 34, (1962), p. 314.

9. Hardrath, H.J., and McEvily, A.J., "Engineering Aspects of Fatigue Crack Propagation," Crack Propagation Symposium, Coll. of Aer. and Roy. Aero. Soc., Cranfield, September 1961.

10. Throop, J.F., "Overload Effect on Fatigue Crack Propagation," Technical Note Prepared for Submission to ASTM Committee E-9 on Fatigue, March 1967.

11. McMillan, J.C., and Hertzberg, R.W., "The Application of Electron Fractography to Fatigue Studies," Electron Fractography, ASTM. STP 436, (1968), p. 89.

12. Forsyth, P.J.E. and Ryder, D.A., "Some Results of the Examination of Aluminum Alloy Specimen Fracture Surfaces," Metallurgia, vol. 63, (1961), p. 117.

13. Stubbington, C.A., "Some Observations on Air and Corrosion Fatigue of an Aluminum-7.5% Zinc 2.5% Magnesium Alloy," Metallurgia, vol. 68, (1963), p. 109.

14. Beachem, C.D., "Electron Fractographic Studies of Mechanical Fracture Processes in Metals," Trans. ASME, Journal of Basic Engineering, 1964.

15. Pelloux, R.M.N., "Fractographic Analysis of the Influence of Constituent Particles on Fatigue Crack Propagation in Aluminum Alloys," Trans. ASM, vol. 57, no. 2, (1964), p. 511.

16. Hertzberg, R.W., and Paris, P.C., "Application of Electron Fractography and Fracture Mechanics to Fatigue Crack Propagation," Proceeding of the First International Conference on Fracture, vol. 1, (1965), p. 459.

17. Taylor Lyman, ed., Metals Handbook, ASM, Metals Park, Ohio, 8th ed., (1961), p. 940.

18. McClintock, F.A., and Pelloux, R.M.N., "Crack Extension by Alternating Shear," Boeing Scientific Research Labs., Seattle, Wash., Feb. 1968.

# Vita

Eric F.J. von Euw was born October 18, 1945 in Buenos Aires, Argentina to Adolph and Eleonora (Grismeyer) von Euw. He received his elementary and part of his secondary education in the Colegio Aleman Alexander von Humboldt school in Mexico City, Mexico and was graduated from C.E. Hughes High School in New York City in 1962.

In June, 1966, Mr. von Euw was graduated from The Cooper Union with a degree of Bachelor of Engineering in Mechanical Engineering, where he was mentioned in the Dean's List.

Since September, 1966, Mr. von Euw has continued his studies at Lehigh University as a research assistant under Dr. R.W. Hertzberg and Dr. R. Roberts on NSF grant number GK 1225.